Probabilistic Power Flow Simulation allowing Temporary Current Overloading

Wander Sybe Wadman
CWI Amsterdam
The Netherlands
w.wadman@cwi.nl

Gabriël Bloemhof
DNV KEMA Energy & Sustainability
Arnhem, the Netherlands
gabriel.bloemhof@kema.com

Daan Crommelin
CWI Amsterdam
The Netherlands
daan.crommelin@cwi.nl

Jason Frank
CWI Amsterdam
The Netherlands
j.e.frank@cwi.nl

***Abstract*—This paper presents a probabilistic power flow model subject to connection temperature constraints. Renewable power generation is included and modelled stochastically in order to reflect its intermittent nature. In contrast to conventional models that enforce connection current constraints, short-term current overloading is allowed. Temperature constraints are weaker than current constraints, and hence the proposed model quantifies the overload risk more realistically. Using such a constraint is justified the more by the intermittent nature of the renewable power source.**

Allowing temporary current overloading necessitates the incorporation of a time domain in our model. This substantially influences the choice of model for the renewable power source, as we explain. Wind power is modelled by use of an ARMA model, and appropriate accelerations of the power flow solution technique are chosen. Several IEEE test case examples illustrate the more realistic risk analysis. An example shows that a current constraint model may overestimate these risks, which may lead to unnecessary over-investments by grid operators in grid connections.

***Keywords*- Probabilistic power flow, renewable generation, Monte Carlo, reliability analysis**

I. Introduction

Renewable energy generation is increasingly integrated, but high penetration of renewable generators is expected to strain the power grid. The limited predictability of distributed renewable sources implies that substantial implementation in the grid will result in a significantly increased risk of power imbalances. Uses of storage, trade or unit commitment may mitigate these risks. Above all, a quantitative uncertainty analysis of the power flow has to be performed, which is the topic of this paper.

An electricity network should fulfill the following constraints:

- The absolute voltage should be between acceptable bounds at all nodes. Formally stated,

$$V_{\min} < |V(t)| < V_{\max} \tag{1}$$

  should hold at all nodes for all times t.
- The reactive power should be between acceptable bounds at all generation nodes:

$$Q_{\min} < Q(t) < Q_{\max}, \tag{2}$$

  should hold at all nodes for all times t.
- The temperature of each connection should be bounded:

$$T(t) \quad < \quad T_{\max}, \tag{3}$$

  should hold at all node connections for all times t. $T_{\max}$ is assumed to be the critical temperature of the connection above which operation failure or degradation over time may occur.

A straightforward method to satisfy the latter constraint, is to ensure that the current never exceeds a certain maximum. That is,

$$|I(t)| \quad < \quad I_{\max}, \tag{4}$$

should hold at all node connections for all times t. In this paper, we assume that $I_{\max}$ corresponds to $T_{\max}$ in the sense that if $I(t) = I_{\max}$ for all times t, then

$$\lim_{t\to\infty} T(t) = T_{\max}. \tag{5}$$

These maxima depend on the material and thickness of the connection. Tables displaying this correspondence for cables can be found in [1], for example.

However, the transient temperature adjustment incurs some lag time, so a mild violation of a given current maximum—with a short duration—may not lead to violation of the temperature constraint. Hence, directly imposing the current constraint may be too restrictive. In fact, the grid dimensioning should anticipate the most extreme event, which may very well be accidental and of short duration. Underestimating the connection capacities in this way, may lead to over-investments in grid connections. Therefore, this article will treat an improved "soft" current constraint, which basically demands that the current be not too high for too long, by focusing on constraint (3) instead of (4).

To include renewable generation units, one must model their uncertain nature. The choice of model should be consistent with available data. Often, and especially when considering investments in new infrastructure, power generation data are scarce, and data of their meteorological sources (e.g. wind speed, solar radiation) are preferred because of their wide availability. Further, the power generation and therefore the connection currents exhibit time correlation. This means that checking for short-term current overloading necessitates the inclusion of chronology in our model, which discourages the

choice for frequency domain approaches [2], [3], [4]. Instead, we prefer a model which involves time correlation of the meteorological sources.

A second reason for proposing a time domain based model is the possible inclusion of storage devices. In order to know the storage capacity and maximum power at some time step, the state of charge information is required. This information will depend on the device behaviour at the previous time step, again necessitating the introduction of chronology into the model. Since storage is one of the main solutions proposed to mitigate the very problem of highly variable renewable power generation, the possibility to extend the model with storage is a welcome feature. Furthermore, we will show that the theoretical benefit of mitigation will be underestimated by use of the current constraint, which implies that storage mitigation is even more promising.

Monte Carlo techniques are one way to quantify the risk of violating the three mentioned constraints. In a straightforward approach, one would first sample the meteorological source. Then the corresponding power injection would be used in a steady state power flow problem. In this way, many power flow solution samples are drawn, after which the risk of constraint violation can be estimated statistically.

This paper elaborates on this approach, using wind power as the straining renewable resource. First, Section II-A presents a time integration scheme for the dynamic connection temperature. Section II-B describes a stochastic wind power simulation method. In Section II-C, we investigate an efficient solver for the steady state power flow problem. Simulation results are presented in Section III. After proposing possible extensions in Section IV, we conclude this paper in Section V.

II. Methodology

A. Short-term overloading

Short-term overloading may warm up a connection insufficiently to increase the temperature to dangerous levels. In fact, the actual quantity to be controlled is the connection temperature $T(t)$, and not the current itself. Fortunately, as is well-known [5], the transient temperature of the connection is described by a first order ordinary differential equation:

$$\tau \frac{\mathrm{d}\Theta(t)}{\mathrm{d}t} + \Theta(t) = \frac{|I(t)|^2}{I_{\max}^2}, \tag{6}$$

with

$$\Theta(t) = \frac{T(t) - T_0}{T_{\max} - T_0}. \tag{7}$$

Here, T_0 denotes the ambient temperature and $I(t)$ the current. The other three coefficients are determined by the connection properties: τ denotes the thermal time constant for the heating of the conductor, whereas $T_{\max}$ and $I_{\max}$ are as defined in Section I.

The solution of (6) is obtained by direct integration:

$$T(t) = T_0 + \frac{T_{\max} - T_0}{\tau I_{\max}^2} \int_0^t |I(s)|^2 e^{(s-t)/\tau} ds. \tag{8}$$

To qualitatively demonstrate to what sense a temperature constraint weakens the current constraint, let us first assume a constant current $I(t) \equiv I$. In this case, the formula above simplifies to

$$T(t) \quad = \quad T_0 + \frac{|I|^2}{I_{\max}^2}\big(T_{\max} - T_0\big)\big(1 - e^{-t/\tau}\big). \tag{9}$$

Practically, this equation states that in order to satisfy constraint (3), one requires

$$1 - \frac{I_{\max}^2}{|I|^2} < e^{-t/\tau} \quad \forall\ t. \tag{10}$$

This inequality naturally shows that no excessive temperature can occur as long as $|I| < I_{\max}$. Otherwise, I is allowed to take on some (constant) value higher than $I_{\max}$ for a maximum duration of

$$-\tau \ln\left(1 - \frac{I_{\max}^2}{|I|^2}\right), \tag{11}$$

as long as the current subsequently drops below $I_{\max}$.

In reality, $I(t)$ is neither constant in time nor known analytically, so we cannot find the analytic solution of (6). However, suppose that we obtain a numeric sample path for $I(t)$. Then we can construct a corresponding sample path for the temperature, by discretizing (6):

$$\tau \frac{\Theta_t - \Theta_{t-\Delta}}{\Delta} + \Theta_{t-\Delta} = \frac{|I_t|^2}{I_{\max}^2}. \tag{12}$$

Here, Θ_t and I_t denote the numerical approximation for $\Theta(t)$ and $I(t)$, respectively, and Δ is the time step. Solving this equation for Θ_t yields a numerical scheme for the relative temperature $\Theta(t)$, and thus for the absolute temperature $T(t)$. In order to fufill the temperature constraint, $\Theta_t < 1$ should hold for all t.

B. ARMA based wind power model

In this article, we will choose wind power as the intermittent power resource. To check the time dependent temperature constraint (3), we require a time domain for the wind speed model. Secondly, the model should capture the wind speed distribution as observed in nature, which is assumed to be the Weibull distribution. Further, to reflect inertia and recurrence of meteorological systems, spatial correlation between meteorological sources as well as temporal periodicity should be incorporated. The autoregressive moving-average (ARMA) model is a well-known technique to fulfill these requirements. The authors of [6] elaborate on an ARMA-GARCH wind speed time series model and demonstrate that the simulated times series realistically represent wind speed observations. For simplicity, we use an ARMA model, thus using the model in [6] except that homoscedasticity is assumed. The autoregressive moving-average model captures the time correlations naturally. The Weibull distributed nature of the wind speed is preserved: the input wind data are first transformed from Weibull realizations to standard normal realizations. On these transformed data, an ARMA(1,1) model is fitted. Parameters are estimated using a standard statistical tool in MatLab

(armax). New time series samples, simulated from this model, are then transformed back to Weibull samples. The daily periodicity is automatically attained by fitting different Weibull cdf's to each hour of the day. The yearly periodicity can be incorporated as well, but is neglected as we consider time series of no longer than one month.
Spatial dependency of wind speeds at different nodes is estimated from the residuals as fitted to the transformed data. The model in turn imposes this dependency by simulating correlated white noise terms: consider the vector of white noise terms $Y \in \mathbb{R}^m$ at a specific time step of a specific Monte Carlo sample, where its elements correspond to all m wind farm locations in the network. Suppose first that we desire the white noise to be a multivariate normally distributed random variable with zero mean:

$$Y \sim \sigma\mathcal{N}(0, \Sigma), \tag{13}$$

with $\sigma > 0$ the desired standard deviation and $\Sigma \in \mathbb{R}^{m\times m}$ the correlation matrix exhibiting the spatial wind speed dependence. Then we sample the multivariate standard normal random variable $Z \sim \mathcal{N}(0, I)$ with independent elements, and perform a Cholesky decomposition $\Sigma = LL^\top$, with $L \in \mathbb{R}^{m\times m}$ lower triangular. By setting

$$Y := \sigma LZ, \tag{14}$$

Y will indeed be a multivariate normally distributed with mean zero, standard deviations σ and correlation matrix Σ. Alternatively, we may desire a multivariate Student's t-distributed random variable Y_k as white noise, where all elements have k degrees of freedom and where the same dependence structure is assumed. In this case, we extend the above procedure by independently sampling a chi-squared distributed random variable v with k degrees of freedom, and set

$$Y_k := Y\sqrt{k/v}. \tag{15}$$

Then Y_k is as desired (more details can be found in [7]).
One month of hourly wind speed measurements from the KNMI[1] [8] are used as data.. For a specific wind turbine, the relation between the wind speed and the wind power is known, as illustrated in Fig. 1. We transform wind speed time series by use of this function, thus obtaining wind power time series.

C. Accelerated power flow method

In order to achieve a satisfactory accuracy level for a connection reliability analysis, one should use a realistic time frame as well as a sufficient number of Monte Carlo samples. Then, for each time step and each Monte Carlo sample, a steady state power flow problem has to be solved. This means that each power flow problem should be solved reasonably fast. This requirement will drive the choice of power flow method.

[1]Koninklijk Nederlands Meteorologisch Instituut. The wind speed at each hour is estimated by the last 10 minutes mean wind speed of the previous hour, in open landscape at 10 meters height

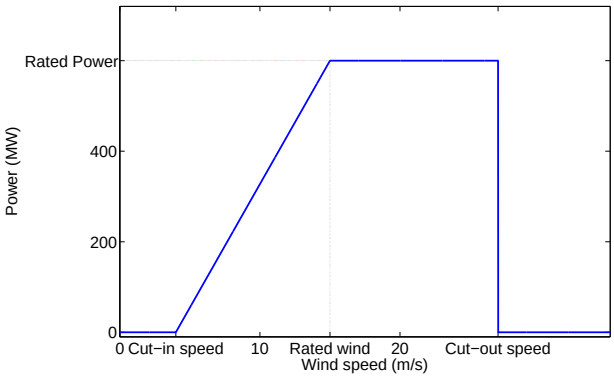

Figure 1. Wind power as function of the wind speed.

A steady state power flow problem involves the solution of the power balance equations:

$$P_i = \sum_j^N |V_i||Y_{ij}||V_j|\cos(\psi_{ij} + \delta_j - \delta_i), \tag{16}$$

$$Q_i = -\sum_j^N |V_i||Y_{ij}||V_j|\sin(\psi_{ij} + \delta_j - \delta_i). \tag{17}$$

Here, $P_i, Q_i \in \mathbb{R}$ denote the active and reactive power, respectively, injected at node i. $|V_i|, \delta_i \in \mathbb{R}$ denote the voltage magnitude and angle, respectively, in grid node i. $|Y_{ij}|, \psi_{ij} \in \mathbb{R}$ denote the absolute value and angle, respectively, of the connection admittance between nodes i and j. N is the number of grid nodes. This nonlinear system of equations has to be solved for the state vectors $|\boldsymbol{V}|$ and $|\boldsymbol{\delta}|$, which is normally done using a Newton-Raphson method [9].
The Fast Decoupled Load Flow (FDLF) method [10] speeds up the conventional method, mainly by assuming approximations which ensure that the Jacobian depends on the admittance matrix Y only. This implies that the Jacobian will be constant in the Newton-Raphson iteration number, and it thus has to be inverted only once. This feature is particularly beneficial in our proposed Monte Carlo method, since the inverse can be reused for all samples.
Elements of the admittance matrix Y are zero precisely when there is no edge between the corresponding nodes. The number of edges in a typical power grid topology is on the order of the number of grid nodes. This means that Y is typically sparse, as is illustrated in Fig. 2, based on two IEEE-test cases [11]. This sparsity can be used to accelerate computations. The nodal power estimates in one Newton-Raphson iteration are computed from the state vectors using (16) and (17). For example, we can rewrite the first equation as

$$P_i/|V_i| = \sum_j |Y_{ij}V_j|\cos(\psi_{ij} + \delta_j - \delta_i), \tag{18}$$

for all nodes i, or in vector form:

$$\boldsymbol{P}/|\boldsymbol{V}| = A(Y, \boldsymbol{\delta})|\boldsymbol{V}|. \tag{19}$$

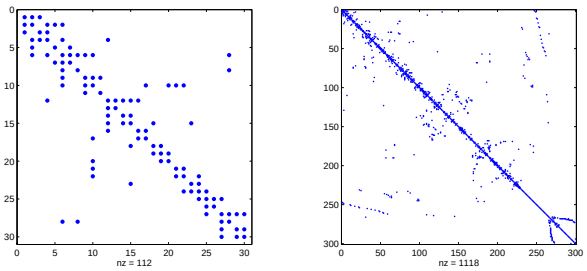

Figure 2. Sparsity of admittance matrix of IEEE-30 and IEEE-300 cases.

Here, $\boldsymbol{P}, \boldsymbol{V}, \boldsymbol{\delta} \in \mathbb{R}^N$ are vectors, the division on the left-hand side is performed elementwise, and the matrix $A(Y, \boldsymbol{\delta}) \in \mathbb{R}^{N\times N}$ depends on Y and $\boldsymbol{\delta}$:

$$A = (a_{ij}), \quad \text{with} \quad a_{ij} = |Y_{ij}| \cos(\psi_{ij} + \delta_j - \delta_i). \qquad (20)$$

Now note that A will be as sparse as Y. Therefore, to evaluate (19), it will be beneficial to compute only the necessary terms in the summand by precaching the indices of nonzero elements of Y. Then, we use the necessary elements of $\boldsymbol{\delta}$ to update the necessary elements of A. In this way, significantly fewer computations have to be performed in this computation step.

Another acceleration for the power flow method involves the power flow solution from the previous time step. Since the amount of renewable power is a piecewise continuous function of time, one may expect that two subsequent solutions will be close. Therefore, the previous solution will be a reasonable first guess for the current problem.

The three acceleration techniques discussed above (i.e. use of FDLF method, sparse computations, and smart initialization) significantly speed up the Newton-Raphson iteration loop. Table I gives an impression of the CPU times[2] of some standard IEEE-test cases: the test case number corresponds to the number of grid nodes. All average CPU times are based on 1000 trials, and a Newton-Raphson tolerance error of 10^{-5} is used. The table clearly shows that a sparse FDLF method is accelerating the conventional power flow method, especially for large grids. Smart initialization may yield some further acceleration, depending on the test case.

We conclude that the computational time for a steady state power flow is on the order of milliseconds. This order of magnitude is desirable, since an accurate uncertainty analysis requires a large number of Monte Carlo samples, each of which involves as many steady state power flow problems as the number of time steps.

[2]MATLAB Version 7.12.0.635 (R2011a), on an Intel(R) Core(TM) i7 CPU M 640 2.80GHz, 2.79 GHz, 3.24 GB of RAM.

Table I
THE AVERAGE CPU TIME (MS) OF A SOPHISTICATED POWER FLOW METHOD IS ON THE ORDER OF MILLISECONDS.

IEEE-test case (# nodes)	**14**	**30**	**57**	**118**	**300**
Conventional power flow	0.96	1.66	4.0	12.3	116.4
FDLF, sparse	0.72	0.78	1.5	2.2	11.6
FDLF, sparse, smart initialization	0.57	0.76	1.5	1.1	11.9

III. RESULTS

A. Comparison between current and temperature constraint

To demonstrate the use of the temperature constraint in a time domain based model, we consider the IEEE-14 test case [11]. The conventional generators at nodes 3 and 6 are replaced by wind farms with comparable rated power (4 base MVA). Wind power time series samples are generated 1000 times, on an interval of one month, on an hourly basis, using spatially correlated KNMI wind speed measurements during August 2011 at Valkenburg and IJmuiden, the Netherlands. Consumption is assumed constant in time. For simplicity, we choose $I_{\max} = 3.7 I_{base}$ uniformly at all connections. Precisely this value is used since then the current exceeds this maximum at some connection approximately once a year. We choose $\tau = 3$ hours (see [12] for realistic values of the thermal time constant).

In our results, the current overloading occurs most of the times at the same connection during periods of high values of wind power generation. Fig. 3 shows an example of temporary overloading at this critical connection, when the temperature constraint is not violated. One can see that the temperature time series is indeed following the current time series. However, local temperature peaks are lower, less frequent and smoother than local current peaks, and slopes are more gradual. This illustrates the "softness" of temperature constraint (3) compared to current constraint (4).

In the upper graph of Fig. 4, all 1000 current time series samples at the critical connection are displayed. In the lower graph of the same figure, the corresponding temperature time series are displayed. One can see from this figure that the current and temperature indeed exceed their maximum only

Table II
THE AUTOREGRESSIVE COEFFICIENT ϕ AND MOVING-AVERAGE COEFFICIENT θ OF THE ARMA(1,1) MODELS AT THE TWO WIND NODES.

	ϕ	θ
Valkenburg	0.94	-0.34
IJmuiden	0.93	-0.15

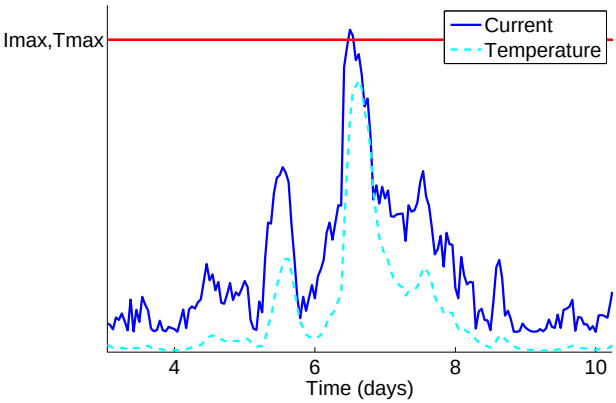

Figure 3. Example: temporary current overloading, which is allowed since the temperature constraint is fulfilled. τ = 3.

Table III
NUMBER OF CONSTRAINT VIOLATIONS FOR DIFFERENT IEEE TEST CASES. 1000 TIME SERIES SAMPLES OF 1 MONTH, $\tau = 3$

Test cases	IEEE-14	IEEE-30	IEEE-57	IEEE-118
Current Violations	88	69	152	101
Temperature Violations	6	16	20	16

rarely. The graph magnification in Fig. 5 clearly illustrates that a current overload does not necessarily imply excess temperature at this connection. This result can be extended to the other connections. In fact, in total 88 current violations were incurred over all samples, which indeed corresponds to approximately once a year. In contrast, the temperature exceeds $T_{\max}$ only 6 times. Other IEEE test cases yield similar results, as can be seen in Table III.

B. Sensitivity to τ

It is clear that the higher the thermal time constant τ, the more the grid capacity will be underestimated when checked by use of current constraints. Table IV shows a quantification estimate of this sensitivity. We repeated the simulation of the previous subsection for different values of τ. The table suggests that our proposed model will yield a significantly more accurate reliability estimate for $\tau > 1.5$. For values of τ close to the time step $\Delta = 1$, our discrete model loses its ability to detect any differences. To explain this, note that for $\tau \to \Delta$, equation (12) goes to:

$$\Theta_t = \frac{|I_t|^2}{I_{\max}^2}, \tag{21}$$

and thus becomes independent of the previous time step. This model phenomenon is partly realistic. On the one hand, the decreasing difference between the two constraints indeed corresponds to reality: τ reflects the time the temperature requires to reach $1 - 1/e = 63.2\%$ of its asymptotic value, in case of constant current. So for small values of τ, the temperature will be close to its asymptotic value, which will cause the two constraints to agree. On the other hand, the total agreement between current and temperature constraints is an overestimation. Current peaks with a duration less than the time step size do not necessarily violate the temperature constraint in reality, in contrast to our model which regards the current as constant during one time step Δ. Therefore, the number of temperature violations in Table IV is overestimated. Since hourly based data limit us to a time step of one hour, this overestimation cannot be reduced by choosing a smaller time step size. It therefore makes no sense to choose $\tau < \Delta$ in the model, whereas the overestimation can be reduced by acquiring data with a smaller time step.

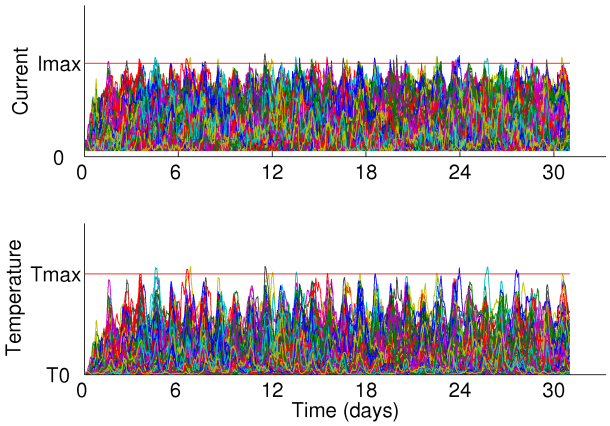

Figure 4. The current and temperature at the critical connection, 1000 time series samples, τ = 3.

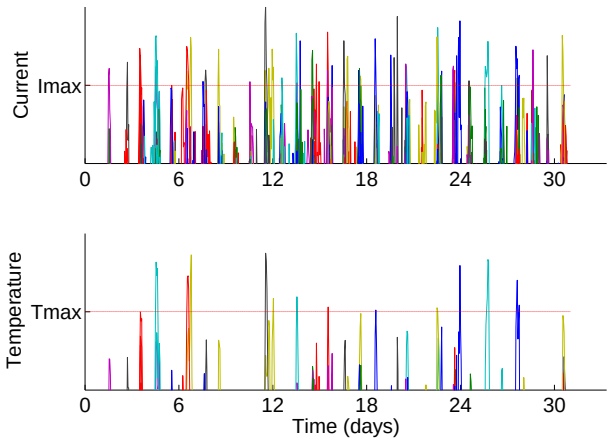

Figure 5. Magnification of Fig. 4: the temperature constraint is violated less frequently than the current constraint.

IV. FURTHER RESEARCH

We aim to extend the model with distributed storage devices, in order to investigate their potential mitigating effect on variable power flows. In fact, Fig. 4 and Fig. 5 suggest that the theoretical benefit of grid mitigation is expected to be substantially higher when estimated using the temperature constraint rather than the current constraint. Specifically, the mean current of all time series is 24% of $I_{\max}$, whereas the mean temperature is only 8% of $T_{\max}$. In other words, the peaks that can be mitigated by use of decentralized storage are relative to the mean even more extreme than conventionally estimated. This implies that mitigation can theoretically increase the connection ampacity by an even higher factor than estimated using the current constraint. Note that mitigation during one time step increases this ampacity even more (although to an extent which is not estimable by our model).
Since storage devices produce and consume, and both to varying degrees, the uncertain nature of their strategies makes

Table IV
NUMBER OF CONSTRAINT VIOLATIONS IN THE IEEE-14 TEST CASE AS FUNCTION OF τ. 1000 TIME SERIES SAMPLES OF 1 MONTH.

τ **(hours)**	1	1.5	2	3	4	5	6
Current Violations	119	80	100	88	95	100	101
Temperature Violations	119	50	25	6	3	0	0

such an extension challenging. Further, we aim to increase the efficiency of the Monte Carlo technique, to achieve higher accuracy with the same number of simulations. We already explained the computational intensity of the proposed model, so an extension with storage devices will definitely necessitate an increase of computational efficiency.

A time frame of one year may simply be incoorporated in the model by iterating the work of this paper twelve times. In this way, the model will automatically exhibit approximate yearly periodicities, since each month model will be calibrated separately.

Other forms of renewable generation may be included in the model as well. Suppose that the characteristics of the considered meteorological source are known, data are available and the relation between the source and power parameters is known. Then one may try to fit an ARMA model and simulate power generation as done in Section II-B. Note that the proposed model can be applied to transportation networks as well as to distribution networks. Finally, stochastic, time-varying consumption can be analogously included.

V. Conclusion

Due to the implementation of uncertain energy generators in power grids, grid operators require quantitative uncertainty analysis of power flow. Grids should satisfy certain constraints in order to match the demand while controlling overload risks. Using a conventional current constraint for grid connections, Monte Carlo simulations underestimate the grid capacity. Instead, a temperature constraint quantifies the risk more accurately. Especially for connections with a high thermal time coefficient, the temperature constraint estimate for overloading frequency may be many times smaller than the current constraint estimate. Therefore, using a model allowing for temporary overloading may save costs by avoiding over-investments.

Acknowledgment

Special thanks go out to DNV KEMA Energy & Sustainability for sharing their experience and their fruitful assistance on the practical side of this research.

References

[1] XLPE, "XLPE land cable systems - user's guide ABB Group," http://www.abb.com/global/scot/scot245.nsf/veritydisplay/ab02245fb5b5ec41c12575c4004a76d0/$file/xlpe%20land%20cable%20systems%202gm5007gb%20rev%205.pdf, 2010, accessed August 31, 2011.

[2] G. Papaefthymiou and B. Klöckl, "MCMC for wind power simulation," *IEEE Transactions on Energy Conversion*, vol. 23, no. 1, pp. 234–240, 2008.

[3] P. Luickx, W. Vandamme, P. Pérez, J. Driesen, and W. D'haeseleer, "Applying Markov chains for the determination of the capacity credit of wind power," in *6th International Conference on the European Energy Market (EEM)*. IEEE, 2009, pp. 1–6.

[4] J. Ehnberg and M. Bollen, "Generation reliability for small isolated power systems entirely based on renewable sources," in *Power Engineering Society General Meeting*. IEEE, 2004, pp. 2322–2327.

[5] H. Pender and W. Del Mar, *Electrical engineers' handbook*. Wiley, 1949, vol. 2.

[6] A. Lojowska, D. Kurowicka, G. Papaefthymiou, and L. van der Sluis, "Advantages of ARMA-GARCH wind speed time series modeling," in *11th International Conference on Probabilistic Methods Applied to Power Systems (PMAPS), 2010 IEEE*. IEEE, 2010, pp. 83–88.

[7] G. Torrent-Gironella and J. Fortiana, "Simulation of high-dimensional t-Student Copulas with a given block correlation matrix," 2005, unpublished.

[8] "Hourly data of the weather in the netherlands," http://www.knmi.nl/klimatologie/uurgegevens/, accessed August 5, 2011.

[9] J. Grainger and W. Stevenson, *Power system analysis*. McGraw-Hill, 1994, vol. 621.

[10] B. Stott and O. Alsac, "Fast decoupled load flow," *Power Apparatus and Systems, IEEE Transactions on*, vol. 1, no. 3, pp. 859–869, 1974.

[11] E. E. University of Washington, "Power systems test case archive," http://www.ee.washington.edu/research/pstca/, 2006, accessed July 12, 2011.

[12] "Thermal overload protection of cables," http://siemens.siprotec.de/download_neu/applications/SIPROTEC/english/Appl_07_Thermal_Overload_Protection_en.pdf, 2005, accessed August 3, 2011.